Landslide Susceptibility Mapping Using GIS and Bivariate Statistical Models in Chemoga Watershade, Ethiopia

Abinet Addis (AbinetAddis2002@gmail.com)
University of Debre markos

Research Article

Keywords: Landslide Susceptibility Mapping (LSM), GIS, Bivariate statistical, Chemoga, Ethiopia

Posted Date: December 13th, 2022

DOI: https://doi.org/10.21203/rs.3.rs-2319713/v1

Abstract

In this study, landslide susceptibility mapping was carried out for Chemoga watershade upper Abay basin in Ethiopia using a bivariate statistical models of Frequency Ratio (FR) and Information Values (IV). The main objective of this study is to identified landslide susceptibility areas using GIS and Bivariate Statistical Models. Based on Google Earth imagery and filed survey, about 169 landslides were identified and classified randomly into training landslides datasets (70%) and the remaining (30%) of landslides datasets were used for validation purpose. The 10 landslides conditioning factors like slope, elevation, aspect, curvature, Topographic Wetness Index, Normalized Difference Vegetation Index, road, river, land use and rainfall were integrated with training landslides to determine the weights of each landslide conditioning factor and factor classes using both frequency ratio and information value models. The landslide susceptibility maps were produced by overlay the weights of all the landslide conditioning factors using raster calculator of the spatial analyst tool in ArcGIS 10.4. The final landslide susceptibility maps were reclassified as very low, low, moderate, high and very high susceptibility classes both FR and IV models.This susceptibility maps were validated using landslide area under the curve (AUC). The results of AUC accuracy models showed that the success rates of the FR and IV models were 0.870 and 0.901, while the prediction rates were 0.880 and 0.923 respectively. The outcome of this paper will help decision-makers for land use planning and landslide mitigation purpose in this study area.

1. Introduction

Landslides are one of the natural hazards causing a lot of casualties and property losses of all over the world [1] [2]. Natural hazards such as landslides, flood, earthquake and drought risk cannot be avoided completely but the processes and consequences can be mitigated [3][4]. Landslides are more widespread than any other geological event, and can occur anywhere in the world. They occur when large masses of soil, rocks or debries move down a slope due to the effect of a natural phenomenon or human activity [5][6].

In Ethiopia landslides, mostly manifested as rock fall, earth slide, debris and mudflow are among the major geo-hazard, especially in the steep and hilly areas of the highlands with greater than 1500m altitude [7][8]. According to [9], from 1960 to 2010 about 388 people are reported dead, 24 injured and a great deal of agricultural lands, houses and infrastructures were affected. The occurrence of landslides is extremely complex phenomenon which depends upon various factors such as geologic structure, lithological association, topography, rainfall, earthquake, and human activity [10]. One of the most widely used approaches to reduce the landslide damages is preparing a landslide susceptibility mapping using suitable models and selecting the effective conditioning factors [11][12]. Over the last decades, many studies have been used different models to prepare landslide susceptibility mapping. These models include the frequency ratio model [13][4][14][15] [16][17][2][18]. A combination of both frequency and Shannon entropy have been applied for landslide susceptibility mapping [19][20][21][22][23][24], Weights of evidence model [25][12][26][27][28][29],Shannon entropy model [30][31][32][11][33]. Landslide susceptibility models based on the bivariate frequency and Weights of evidence models [34] and frequency ratio and information value models [35][1][10]. Landslide susceptibility models based on the bivariate frequency ratio and multivariate logistic regression models [36][37][38][39][40] are used with the development of GIS techniques. Geographical information system platforms help in the calculation and visualization of the cumulative effects of conditioning factors on landslides.

However, each of the above-mentioned methods has certain limitation in terms of landslide susceptibility mapping which may produce various conditions. Therefore, the combination of bivariate (FR and IV) statistical models is

used in this study to fill the limitation of every applied method. FR and IV methods are both bivariate statistical of quantifiable methods in the study of natural hazards. Therefore, the study used FR and IV models with GIS to generate landslide hazard areas to identify the high-risk areas and the most critical conditioning factors responsible for landslides in the study area. The main objective of this study is to identify the landslide susceptibility areas using GIS and the combination of bivariate (FR and IV) statistical models in Chemoga watershed, Upper Abay River basin, Ethiopia. The results map will help the regional and local authorities and decision makers to mitigate the risk of landslide hazard by developing different strategies.

2. Materials And Methods

2.1 Description of the study area

The Chemoga watershed is located in the upper Abay River basin Ethiopia with an area 1414.85km^2. According from UTM coordinate system, the location of watershed is approximately between longitudes 330000m E – 380000m E and latitude 1110000m N – 1170000m N direction as shown in fig. 1. Topographically, the altitude ranges from 863m to 3946m and the slope angle varies from 0 to 67 degrees. In terms of land use, most of the watershed is covered by scrub/shrub and crop lands. The study area receives high amount of rainfall during the summer season. The average recorded annual precipitation and temperature of the area was 1376 mm and 16.95 °C respectively.

2.2 Data source and methodology

In this study, to achieve the main objective was after using primary and secondary data. The primary data were collected from field survey and observation and the secondary data for the study was acquired from governmental and non-governmental institutions, journals, internet and other documents. The main data used for this study were land sentinel 2 images and DEM of the area, Google earth imagery and topographical map of the area. The data layer of land use and NDVI were derived from sentinel 2 images and DEM data used to create the slope, elevation, aspect, curvature, and TWI data layers and their extents through spatial analysis tools. Another data was used in this study, the average annual rainfall of metrological stations was obtained from the National Meteorological Agency of Ethiopia. The main road and river were digitized from the topographical map of Ethiopia. The other data sets of landslides were digitized from the study area of Google Earth imagery and field surveys. All the data layers have been constructed and combined in ArcGIS 10.4 tool. ArcGIS tool was applied throughout the whole process in this study. Accordingly, the FR and IV models were used to generate elaborative landslides susceptibility map. For the purpose of assessment and validation of landslide susceptibility map, the methodology shows in Fig 2.

Table 1: Type of conditioning factors, format and Source

Type conditioning factors	Format	Source
Slope, Elevation, Aspect, Curvature and TWI	Raster	Derived from of DEM image (2021)
Road and River	Vector	Digitized from the study area of Topographic map, Ethiopian Mapping Agency, Addis Ababa, Ethiopia
Land use and NDVI	Raster	Analyzed from Sentinel 2 images in the USGS (2021)
Rainfall	Vector	Interpretation of Ethiopian National Metrological Agency, Addis Ababa (1990 - 2021)
Landslide inventory		Digitized from Google Earth imagery and field survey

2.3 Landslide inventory map

Landslide inventory mapping is the systematic mapping of existing landslides in a region using various techniques such as field survey, aerial photographs or Google Earth imagery interpretation, satellite image interpretation, and literature search for historical landslide records, technical and scientific reports, governmental reports, and the interview of experts [41][42]. In this research, the landslide inventory map which has a total of 169 single landslide locations was created based on Google Earth imagery digitized into points using GIS 10.4 and field visits. Though there is no specific rule for defining how landslide occurrence will be allocated into training and validation data sets [43], usually research work has been done by using 70% of landslides events as training data sets for preparing landslide susceptibility model and the rest 30% have been used for validation of the output model [44][14][11]. In this study, 118 (70%) of the landslides were used to training landslide susceptibility models and the remaining 51 (30%) of the landslides were used to model validation, shown in fig 3.

2.4 Landslide conditioning factors

To identify a landslide occurrence conditioning factors is a very complex phenomenon. Because there is no any standard rule to select which factor to be used or not, rather than deciding on the nature of area and data availability [45]. In this study, ten conditioning factors were selected based on the literatures, effectiveness, availability of data and the relevance with respect to land slide occurrence [23]. These conditioning factors are slope, elevation, aspect, curvature, TWI, NDVI, road, river, land use and rainfall. All the selected conditioning factors were used to perform the landslide susceptibility mapping. Each factor was converted to a raster format and was classified based on Jenks natural breaks method in ArcGIS application.

In landslide susceptibility studies, slope is considered one of the major contributions of landslide conditioning factor of slope failure [21][46]. According to the importance of slope conditioning factor in the landslide occurrence, the study area was classified into five classes in degree. With increase in slope angle, the possibility of landslide occurrence increases [47][48][19]. Elevation is an important conditioning factor in landslide susceptibility mapping and it also impacts the environmental conditions on slopes such as human activity, vegetation, soil moisture and climate [49][50]. Curvature is a key an important role in the surface run off and ground infiltration thus affects the erosion of the surface and ground water condition of the region [17]. The curvature map of the study area was classified into concave (negative), convex (positive) and flat (zero) surfaces. In the case of curvature the more negative the value, the higher the probability of landslide occurrence [29]. Aspect represents the direction that

a slope faces [49]. Slope aspect affects erosion, surface evaporation, desertification, solar heating and surface weathering, thus affecting the occurrence of landslides [46][51]. Topographic wetness index (TWI) is among one of the important factors responsible for the landslide, which can quantitatively display the control of terrain on the spatial distribution of soil moisture, is a widely used terrain attribute. The TWI conditioning factor was obtained from DEM with 30m spatial resolution by equation (1) to express as follows:

$$TWI = Ln (A_s/\tan \beta) \quad (1)$$

Where, A_s is the specific catchment area (m^2/m) and β is slope angle in degrees [52]. TWI is used to measure topographic control of hydrological procedures [53]. Rainfall is considered to be one of the landslides occurrences a conditioning factor. Rainfall map was prepared using station locations in the study area through the IDW interpolation method of annual average precipitation (1990 - 2021). Road is one of the most effective factors on landslide occurrence [1]. Road construction near the hillside may lead to changes in the natural conditions of areas. River networks plays an important role in landslide occurrence factor closely to surface water. The NDVI conditioning factor was obtained from Sentinel-2 satellite imagery with 30m spatial resolution by equation (2) to express as follows:

$$NDVI = \frac{IR-R}{IR+R} \quad (2)$$

Where, IR is the infrared and R is the red bands of the electromagnetic spectrum. NDVI values between −1.0 and 1.0, where any negative values are mainly generated from clouds, water, and snow and values near zero are mainly generated from rock and bare soil and the positive value indicates that the ground is covered by vegetation. Land use is an important conditioning factor that affects the occurrence of landslides. The map of land use was derived from Sentinel-2 satellite imagery, by using a supervised classification technique in ArcGIS. The land use map was classified in to six classes. The study area is predominantly covered with the cropland and scrubs.

2.5. Landslide Susceptibility Modeling

2.5.1 Frequency Ratio model

Frequency ratio is one of the most widely adopted and popular methods for landslide susceptibility assessment [16] [14]. FR is one of the most cited bivariate statistical analysis methods in natural hazard studies, like flood, landslide and drought hazards [56]. The frequency ratio is the ratio of the area where landslides occurred in the total study area and also is the ratio of the probabilities of a landslide occurrence to a non-landslides occurrence for a given attribute [57][58]. Generally, a greater ratio indicates a stronger relationship between a conditioning factor and landslide and vice versa. A value of 1 is an average value for the area landslides occurring in the total area. If the FR value is greater than 1 indicates a high probability of landslide occurrence, and a value less than 1 indicates a low relationship between probabilities of landslide occurrence. The landslides susceptibility map (LSM) can be calculated by summing the FR of all of the factors considered equation (3) as follows:

$$LSM = \sum_{j=1}^{n} FR \quad (3)$$

Where *LSM* is landslide susceptibility map and *FR* represents for each factor type or class, *n* is the number of factors. FR was applied the weights were assigned to each class of each conditioning factor. The FR can be obtained by equation (4) as follows:

$$FR= \left[\frac{Npix(SXi)/\sum_{i=1}^{m} SXi}{Npix(Xj)/\sum_{j=1}^{n} Npix(Xj)}\right] \quad (4)$$

where the number of landslide pixels in class i of the factor X is represented by N_{pix} (SX_i); the total number of pixels within factor Xj is represented by $N_{pix}(X_j)$; m is the number of classes in factor X_i; and n is the total number of factors in the study area [58].

2.5.2 Information Value model

The information value (IV) model is a bivariate statistical approach that has the advantage of assessing landslide susceptibility in an objective way from information theory and the model was originally proposed by [54] and later slightly modified by [42]. The information value model is used to evaluate the spatial relationship between the conditioning factor classes and the probability of landslide occurrence. Generally, the higher value of IV model corresponds to the stronger relationship between the probability of landslide occurrence and the conditioning factor class. A value of 0 is an average value for the area landslide occurring in the total area. If the IV value is greater than 0 indicates a high probability of landslide occurrence, and a value less than 0 indicates a low relationship between the probabilities of landslide occurrence. Therefore, the landslide susceptibility map (L*SM*) for each pixel was computed by summing the information values of each factor class as follows:

$$LSM = \sum_{i=1}^{n} IV\ i \quad (5)$$

Where *LSM* is the landslide susceptibility map and *IVi* is the information value each factor class, *n* is the number of factors. IV was applied, and the weights were assigned to each class of each conditioning factor. The information value (IV) can be calculated using the following formula [54].

$$IV= \log (\text{Conditional probability /prior probability}) = \log \left[\frac{Nslpix/Ncpix}{Ntspix/Ntapix}\right] \quad (6)$$

Where *Nslpix* is a number of landslide pixels in a given class, *Ncpix* is the number of pixels in a given class, *Ntspix* is a total number of landslide pixels in the study area, and *Ntapix* is a total number of pixels in the study area.

3. Results And Discussion

3.1 Application of Frequency Ratio (FR) model

FR was measured for each class of every landslide conditioning factor by dividing the landslide occurrence ratio by the area ratio. The results of the FR model for each of the classes of effective factors are shown in Table 2. In general, the FR value of 1 indicates the average correlation between landslide occurrence and effective factors. If

the FR value would be greater than 1, there is a high landslide occurrence and FR value less than 1 indicates that low landslide occurrence [43]. The analysis of FR for the relationship between landslide occurrence and slope degree indicate that class $33^0 – 67^0$, the highest FR value of 9.27 among the other classes of slope degree, it indicating that a high landslide occerence. The remaining classes of slope are a low probabilities of landslide occurrence. In the study area, was observed that when landslide occurrence probability increased as the slope gradient increased up to a certain extent and then, it decreased with results of other literature studies [20]. Because the Higher slope values trigger the effect of gravity and also increase shear stress [42]. According to the relationship between landslide occurrence and elevation factor indicate that, the ranges between 1509m – 2042m with a value of FR is 2.78, which implies a high probabilities of landslide occurrence in the study area. The elevation ranges between 863m -1509m, 2042m – 2513m, 2513m -3059m and 3059m – 3946m, have the lowest FR values (0.28, 0.99, 0.41 and 0.53 respectively), indicating that a low probabilities of landslide occurrence. Commonly, as the elevation increases, the probability of landslide occurrence increases up to a certain extent and then, it decreased. In the case of aspect factor classes are the most abundance on east facing (FR=1.03), south east facing (FR=1.60), south facing (FR=1.24), south west facing (FR=1.42),west (FR=1.24) and northwest (FR=1.04), indicating a high probabilities of landslide occurrence. However, the remaining aspect classes have the lowest abundance of FR value less than 1, it indicates that a low probabilities of landslide occurrence. Considering the case of land use, results show that the water body, forest area, grass and scrub/shrub and bare land use types have values of FR (2.07, 1.50, 1.54 and 22.92 respectively), which implies that a high probabilities of landslide occurrence. The highest FR value of bare land are due to its exposure to erosion and soil moisture [37]. In the case of curvature factor classes of concave (-16.55 – (-0.98)) and convex (0.75 – 20.22), have the highest value of FR (1.39 and 1.38) respectively, indicating a high probabilities of landslide occurrence. Subsequently, at curvature class of flat slope (-0.98 – 0.75), has a low FR value (0.70), indicating that a low probabilities of landslide occurrence. Distance from the road classes 6985m - 11577m with a value of FR (2.05), has the greatest impact on landslide coherence. Commonly, the landslide frequency increases as the distance from roads decreases. Therefore, the existing road and the on-going constructions disturb the stability of slope there by increasing the probability of landslide occurrence with results of other literature studies [19][20]. According to [60], the landslides probability decreases with the increasing distance from river networks. In this study area, distance from river networks, 2560-4133m class exerts the highest influence on landslide occurrence in this study. The reason is that permanent rivers are the main source of moisture for landslide occurrence. In the NDVI, the FR value is greater than one, where the NDVI classes -0.04– 0.10 and 0.23 – 0.48, indicating a high probabilities of landslides occurrence. This class of NDVI means bare land, built up areas and scrubs. However, the remaining NDVI classes have low FR value less than one; with relatively high vegetation coverage can easily lead to landslide occurrence. The relationship between TWI landslide probabilities showed that 2.72 – 5.30, class has the highest value of FR (1.98), greater than one. With regard to the conditioning factor rainfall, three classes with 1484 – 1519mm/yr, 1519 - 1539mm/yr, and 1539 - 1563mm/yr have a higher FR value than the other classes and are the most landslide occurrence classes.

3.2 Application of Information Value model

The information value of each conditioning factor was calculated through equation (5), and the spatial relationship between each conditioning factors and flood occurrence is shown in (Table 2). The relationship is reflected by the IV values of the factor classes. If the factor class of IV value would be negative, there is a low landslide occurrence. On the other hand, if the factor class of IV value would be positive, there is a high probability landslide occurrence [42]. The analysis of IV for the relationship between landslide occurrence and slope degree indicate that class $33^0 – 67^0$ is highly prone to landslide having the highest IV value of 0.967 in high-lying areas, whereas the flat slope showing

less probability of landslide occurrence. It can be indicated that as the slope is higher, the incidence of landslide is high and vice versa. According to the relationship between landslide occurrence and elevation factor indicate that the lower class 1509m – 2042m (IV= 445), which implies a high probabilities of landslide occurrence and all other classes have very less impact on landslide occurrence in the study of area. Generally, the behavior of landslide is mostly occurred on the higher area. In the case of aspect conditioning factor classes are the lowest abundance on flat facing (IV= -0.534), north (IV = -0.434), and northeast (IV= -0.166) indicating a low probabilities of landslide occurrence. However, the remaining aspect classes have the most abundance of IV value is postive, it indicates that a high probabilities of landslide occurrence. Considering the case of curvature, the class of flat has the lowest value of (IV= -0.156), indicating a low probabilities of landslide occurrence in this area. Subsequently, at curvature classes of convex and concave slope have a high value of IV (0.142 and 0.139) respectively, indicating that a high probabilities of flat occurrence. In this study, distance from the road has a highest abundance of IV value is 0.312 the class between 6985 to 11577m, it indicates that a high probabilities of landslide occurrence. But the rest classes are a lower abundance of IV values, it indicates that a low probabilities of landslide occurrence. Commonly, the occurrence of landslide increases as the distance to road decreases. Therefore, the existing road and the on-going constructions disturb the stability of slope there by increasing the probability of landslide occurrence. A high IV value (0.178) for subclass 2560 – 4133m was observed for the factor distance to the river. However, the remaining sub classes have the lowest abundance of IV value is negative, it indicates that a low probabilities of landslide occurrence in this study. In the NDVI, the IV value is positive, where the NDVI classes -0.04 - 0.10, and 0.23-0.48, indicating a high probabilities of landslide occurrence. This class of NDVI means water body and bare lands. However, the remaining NDVI classes have low IV value is negative; with relatively high vegetation coverage can easily lead to landslide occurrence. The relationship between TWI landslide occurrence probabilities showed that 2.72 – 5.30, classe has a positive value of IV is 0.297, it indicates that a higher landslide occurrence. Land use, each class has a different influenced on landslide and settlements and crops land can reduce the landslide. However, forest area, water body, grasses and bare land have a high impact on landslide occurrence in this study. Rainfall is another important conditioning factor for the impact of landslide occurrence shown in (Table 2). The average annual rainfall classes 1484 – 1519mm/yr, 1519 – 1539mm/yr and 1539 – 1563mm/yr have the positive value of IV (0.122, 0.06 and 0.091), respectively, indicating that a high lansslide occurrence. However, the other classes have a negative value of IV (-0.988 and -0.157), indicates that a lower probabilities of landslide occurrence.

Table 2: Spatial relationship between each conditioning factors and landslide occurrence using FR and IV models

Conditioning Factors	Classes	Class Pixels	%Class Pixels	Landslide Pixels	%Landslide Pixels	FR	IV
TWI	2.72 - 5.30	323931	25.08	1594	49.64	1.98	0.297
	5.30 - 6.40	494455	38.28	830	25.85	0.68	-0.171
	6.40 - 7.72	268130	20.76	440	13.7	0.66	-0.18
	7.72 - 9.42	142058	11	260	8.1	0.74	-0.133
	9.42 - 16.72	63073	4.88	87	2.71	0.55	-0.256
Land use	Water body	582	0.05	3	0.09	2.07	0.317
	Forest	59977	4.64	223	6.94	1.5	0.175
	Crops land	639319	49.5	1217	37.9	0.77	-0.116
	Grass/Scrub/Shrub	451440	34.95	1730	53.88	1.54	0.188
	Settlements	139820	10.82	9	0.28	0.03	-1.587
	Bare land	509	0.04	29	0.9	22.92	1.36
NDVI (ratio)	(-0.04)- 0.10	231989	17.96	1007	31.36	1.75	0.242
	0.10 -0.12	458792	35.52	945	29.43	0.83	-0.082
	0.12 - 0.18	367141	28.42	692	21.55	0.76	-0.12
	0.18 - 0.23	180380	13.97	410	12.77	0.91	-0.039
	0.23- 0.48	53345	4.13	157	4.89	1.18	0.073
Road (m)	0 -3253	392519	30.39	752	23.49	0.77	-0.112
	3253 - 6985	327932	25.39	641	20.02	0.79	-0.103
	6985 - 11577	264136	20.45	1342	41.92	2.05	0.312
	11577 - 16936	174099	13.48	380	11.87	0.88	-0.055
	16936 - 24399	133032	10.3	86	2.69	0.26	-0.584
Rainfall (mm/yr)	1484 - 1519	196729	15.23	647	20.15	1.32	0.122
	1519 - 1539	331512	25.67	946	29.46	1.15	0.06
	1539 - 1563	438126	33.92	1343	41.82	1.23	0.091
	1563 - 1593	195465	15.13	50	1.56	0.1	-0.988
	1593 - 1636	129815	10.05	225	7.01	0.7	-0.157
River (m)	0 - 1243	384766	29.79	949	29.55	0.99	-0.003
	1243 - 2560	363147	28.12	787	24.51	0.87	-0.06
	2560 - 4133	304347	23.57	1139	35.47	1.51	0.178
	4133 - 6072	160917	12.46	306	9.53	0.76	-0.116
	6072 - 9327	78320	6.06	30	0.93	0.15	-0.812

Slope (degree)	0 - 7	447188	34.62	263	8.19	0.24	-0.626
	7 - 13	449831	34.83	467	14.54	0.42	-0.379
	13 - 21	244633	18.94	607	18.9	1.00	-0.001
	21 - 33	107403	8.32	892	27.78	3.34	0.524
	33 - 67	42592	3.3	982	30.58	9.27	0.967
Curvature (ratio)	Convex (-16.55 - (-0.98)	248830	19.26	858	26.72	1.39	0.142
	Flat (-0.98 - 0.75)	721286	55.84	1253	39.02	0.7	-0.156
	Concave (0.75 - 20.22)	321531	24.89	1100	34.26	1.38	0.139
Elevation (m)	863 - 1509	334549	25.9	235	7.32	0.28	-0.549
	1509 -2042	216355	16.75	1497	46.62	2.78	0.445
	2042 - 2513	482883	37.39	1190	37.06	0.99	-0.004
	2513 -3059	169167	13.1	172	5.36	0.41	-0.388
	3059 - 3946	88693	6.87	117	3.64	0.53	-0.275
Aspect (direction)	flat (-1)	82464	6.38	60	1.87	0.29	-0.534
	North (0 - 22.5 and 337.5 - 360)	213107	16.5	195	6.07	0.37	-0.434
	Northeast (22.5 - 67.5)	123845	9.59	210	6.54	0.68	-0.166
	East (67.5 - 112.5)	151109	11.7	388	12.08	1.03	0.014
	Southeast (112.5 - 157.5)	158025	12.23	629	19.59	1.6	0.204
	South (157.5 - 202.5)	131648	10.19	407	12.68	1.24	0.095
	Southwest (202.5 - 247.5)	142068	11	502	15.63	1.42	0.153
	West (247.5 - 292.5)	146211	11.32	449	13.98	1.24	0.092
	Northwest (292.5 - 337.5)	143170	11.08	371	11.55	1.04	0.018

3.3 Landslide susceptibility maps

Map of each conditioning factor is prepared with the help of ArcGIS 10.4 and then the frequency ratio values were calculated. The calculated FR values for each pixel in the LSM indicate the relative susceptibility to landslide occurrence. The higher pixel values of LSM have the higher landslide susceptibility while the lower pixel values will have lower susceptibility. The landslide susceptibility map was calculated based on the frequency ratio values that have been determined in the training process that can be added in a raster calculator of ArcGIS 10.4, as follows:

$$FSM = (FR_{slope} + FR_{elevation} + FR_{aspect} + FR_{land\ use} + FR_{curvature} + FR_{road} + FR_{river} + FR_{NDVI} + FR_{TWI} + FR_{rainfall}) \quad (7)$$

The LSM values for the frequency ratio model in the study area range from 14 to 81. These values were classified into five susceptibility classes of very low, low, moderate, high and very high susceptibility using the geometrical interval method for visual interpretation (Fig.5a). From the output of analysis carried out using the ArcGIS 10.4 (table 3), the very low and low susceptibility zones cover 17.36% and 31.86% of the study area respectively, whereas the moderate, high, and very high susceptibility zones cover 27.10%, 17.50%, and 6.18% of the total area, respectively.

The landslide susceptibility map was produced from information value model (Fig. 5b). The simplest landslide susceptibility equation for this model is given as follows:

$$LSM = (IV_{Slope} + IV_{Elevation} + IV_{Aspect} + IV_{Land\ use} + IV_{Curvature} + IV_{road} + IV_{river} + IV_{NDVI} + IV_{TWI} + IV_{Rainfall}) \quad (8)$$

The LSM value varies from -5.59 to 3.91 for information values model. These values were classified into five susceptibility classes of very low, low, moderate, high and very high susceptibility using the Jenks natural breaks method. Then, the very low susceptible zone covers 9.17% of the total study area, whereas low, moderate, high, and very high susceptible zones cover 24.15%, 34.81%, 22.35% and 9.52% of the total area, respectively (Table 3).

Table 3: Landslide susceptibility classes and summery of FR and IV models

Landslide susceptible classes	FR model			IV model		
	Range	Area in (km^2)	Area in (%)	Range	Area in (km^2)	Area in (%)
Very low	14 - 27	245.62	17.36	-5.59 – -2.35	129.73	9.17
Low	27 - 35	450.80	31.86	-2.35 - -1.34	341.72	24.15
Moderate	35 - 43	383.44	27.10	-1.34- -0.45	492.47	34.81
High	43 - 54	247.59	17.50	-0.45 – 0.71	316.20	22.35
Very high	54 - 81	87.40	6.18	0.71 – 3.91	134.72	9.52

3.4 Validation of landslide susceptibility maps

After obtaining the landslide susceptibility maps using FR and IV models, their validation is necessary in order to check their reliability. Without model validation, landslide susceptibility maps will not be meaningful. In the present study, the performance of the LSM produced by FR and IV models, were evaluated using area under the curve (AUC). The area under the curve (AUC) is the measure that indicates the accuracy of the landslide susceptibility maps by creating success and prediction rate curves. The success rate curve represented the model fitness to existing landslide and the comparison of the training dataset with the landslide susceptibility map provides the success rate curve. The prediction rate curve indicates the model efficiency to predict future landslide and the comparison of the

validation dataset with the landslide susceptibility map provides the prediction rate curve [61][43]. For this study, 118 (70%) of the landslides were used to training landslide susceptibility models and the remaining 51 (30%) of the landslides were used to model validation. The success and predictive rate curves can be created for both FR and IV models by using ROC module in ArcGIS 10.4 tool. The AUC rate curves were drawn through the x-axis both the training and validation landslides (true positive rate) and y-axis (false positive rate). The total AUC can be used to determine prediction accuracy of the susceptibility map qualitatively in which larger area means higher accuracy achieved. The AUC value ranges from 0.5 to 1.0 are used to evaluate the accuracy of the model [61]. The qualitative relationship between AUC and prediction accuracy can be classified as follows; excellent (0.9 – 1.0); very good (0.8 - 0.9); good (0.7 - 0.8); average (0.6 - 0.7) and fair (0.5 - 0.6), [61]. If AUC value is close to 1.0, then the model will have ideal performance, where as a value is equal or less than 0.5, then the model will have poor performance [62]. The result showed that, the AUC of the success rate curves were 0.870 for the FR model and 0.901 for the IV model, which be equivalent to 87.00% and 90.10% predication accuracy respectively (Fig 6a). The AUC of the prediction rate curves were 0.880 for the FR model and 0.923 for the IV model, which be equivalent to 88.00% and 92.30% predication accuracy respectively (Fig 6b). The AUC of the success rate and predictive rate curves range between 0.8-0.9, indicating that a very good performance of FR model. Also, the success rate and predictive rate curves range between 0.9-1.0, indicating that excellent performance of IV model. Therefore, based on the calculated AUC, it is clearly that the IV model exhibited better result for landslide susceptibility mapping in this study.

4. Conclusion

In this study, frequency ratio and information value models were used to identify the landslides susceptible areas in Chemoga watershade, Ethiopia. Ten landslides conditioning factors were selected based on the availability and effective data. These factors were slope, elevation, aspect, land use, curvature, road, river networks, NDVI, TWI and rainfall to prepare landslide susceptibility maps. A landslide inventory map was prepared using Google earth imagery and filed survey assessment. For this process, 169 landslide locations were identified and mapped. Also classified into 70% (118) landslides were used to training and 30% (51) of the landslides were used to validation purpose. The susceptibility maps produced by FR and IV models were divided into five susceptibility classes such as very low, low, moderate, high, and very high susceptibility classes based on geometric interval method. The AUC rate curve quantitatively indicates the performance of the susceptibility maps. The model of information value results showed that the accuracies of success rate (90.10%) and predicative rate (92.30%) of the landslide susceptibility map. Similarly, the model of frequency ratio results showed that the accuracies of success rate (87.00%) and predicative rate (88.00%) of the landslide susceptibility map. Finally, this study confirmed that the models of FR and IV were found to be simple, reliable and effective models for landslide susceptibility mapping of the study area. The final output of landslide susceptibility maps can help the decision makers as basic information for the concerned authorities of government and no governmental, district and zonal level of land use planning to perform proper actions in order to prevent and mitigate the existing and future landslides occurrence.

Declarations

Acknowledgements: Thanks to staff of Civil Engineering Department, University of Debre markos, Ethiopia.

Funding

This research was funded by the author

Compliance with ethical standards

Conflict of interest the author declare that they have no conflict of interest

References

1. B. Li, N. Wang, and J. Chen, “GIS-Based Landslide Susceptibility Mapping Using Information, Frequency Ratio, and Artificial Neural Network Methods in Qinghai Province, Northwestern China,” *Adv. Civ. Eng.*, vol. 2021, 2021, doi: 10.1155/2021/4758062.
2. S. C. Pal and I. Chowdhuri, “GIS-based spatial prediction of landslide susceptibility using frequency ratio model of Lachung River basin, North Sikkim, India,” *SN Appl. Sci.*, vol. 1, no. 5, pp. 1–25, 2019, doi: 10.1007/s42452-019-0422-7.
3. P. Gyawali, Y. M. Aryal, A. Tiwari, K. C. Prajwol, and K. Ansari, “Landslide Susceptibility Assessment Using Bivariate Statistical Methods : A Case Study of Gulmi District , western Nepal,” vol. 16, no. Ndrr, pp. 29–40, 2019, doi: 10.36297/vw.jei.v3i2.60.
4. T. H. Mezughi, J. M. Akhir, A. G. Rafek, and I. Abdullah, “Landslide susceptibility assessment using frequency ratio model applied to an area along the E-W highway (Gerik-Jeli),” *Am. J. Environ. Sci.*, vol. 7, no. 1, pp. 43–50, 2011, doi: 10.3844/ajessp.2011.43.50.
5. D. M. Cruden, “A simple definition of a landslide,” *Bull. Int. Assoc. Eng. Geol. - Bull. l’Association Int. Géologie l’Ingénieur*, vol. 43, no. 1, pp. 27–29, 1991, doi: 10.1007/BF02590167.
6. L. Shano, T. K. Raghuvanshi, and M. Meten, “Landslide susceptibility mapping using frequency ratio model: the case of Gamo highland, South Ethiopia,” *Arab. J. Geosci.*, vol. 14, no. 7, 2021, doi: 10.1007/s12517-021-06995-7.
7. G. Mewa and F. Mengistu, “Assessment of Landslide Risk in Ethiopia: Distributions, Causes, and Impacts,” *Landslides*, no. April, 2022, doi: 10.5772/intechopen.101023.
8. C. Tesfa and K. Woldearegay, “Characteristics and susceptibility zonation of landslides in Wabe Shebelle Gorge, south eastern Ethiopia,” *J. African Earth Sci.*, vol. 182, no. November 2020, p. 104275, 2021, doi: 10.1016/j.jafrearsci.2021.104275.
9. M. Meten, N. PrakashBhandary, and R. Yatabe, “Effect of Landslide Factor Combinations on the Prediction Accuracy of Landslide Susceptibility Maps in the Blue Nile Gorge of Central Ethiopia,” *Geoenvironmental Disasters*, vol. 2, no. 1, 2015, doi: 10.1186/s40677-015-0016-7.
10. S. P. Mandal, A. Chakrabarty, and P. Maity, “Comparative evaluation of information value and frequency ratio in landslide susceptibility analysis along national highways of Sikkim Himalaya,” *Spat. Inf. Res.*, vol. 26, no. 2, pp. 127–141, 2018, doi: 10.1007/s41324-017-0160-0.
11. N. D. Dam *et al.*, “Evaluation of Shannon Entropy and Weights of Evidence Models in Landslide Susceptibility Mapping for the Pithoragarh District of Uttarakhand State, India,” *Adv. Civ. Eng.*, vol. 2022, 2022, doi: 10.1155/2022/6645007.
12. Z. Anis, G. Wissem, V. Vali, H. Smida, and G. Mohamed Essghaier, “GIS-based landslide susceptibility mapping using bivariate statistical methods in North-western Tunisia,” *Open Geosci.*, vol. 11, no. 1, pp. 708–726, 2019, doi: 10.1515/geo-2019-0056.
13. D. Thapa and B. P. Bhandari, “GIS-Based Frequency Ratio Method for Identification of Potential Landslide Susceptible Area in the Siwalik Zone of Chatara-Barahakshetra Section, Nepal,” *Open J. Geol.*, vol. 09, no. 12, pp. 873–896, 2019, doi: 10.4236/ojg.2019.912096.

14. Y. xing Zhang, H. xing Lan, L. ping Li, Y. ming Wu, J. hui Chen, and N. man Tian, “Optimizing the frequency ratio method for landslide susceptibility assessment: A case study of the Caiyuan Basin in the southeast mountainous area of China,” *J. Mt. Sci.*, vol. 17, no. 2, pp. 340–357, 2020, doi: 10.1007/s11629-019-5702-6.
15. T. D. Acharya, I. T. Yang, and D. H. Lee, “GIS-based landslide susceptibility mapping of Bhotang, Nepal using frequency ratio and statistical index methods,” *J. Korean Soc. Surv. Geod. Photogramm. Cartogr.*, vol. 35, no. 5, pp. 357–364, 2017, doi: 10.7848/ksgpc.2017.35.5.357.
16. L. Li, H. Lan, C. Guo, Y. Zhang, Q. Li, and Y. Wu, “A modified frequency ratio method for landslide susceptibility assessment,” *Landslides*, vol. 14, no. 2, pp. 727–741, 2017, doi: 10.1007/s10346-016-0771-x.
17. H. J. Oh, S. Lee, and S. M. Hong, “Landslide Susceptibility Assessment Using Frequency Ratio Technique with Iterative Random Sampling,” *J. Sensors*, vol. 2017, 2017, doi: 10.1155/2017/3730913.
18. F. E. S. Silalahi, Pamela, Y. Arifianti, and F. Hidayat, “Landslide susceptibility assessment using frequency ratio model in Bogor, West Java, Indonesia,” *Geosci. Lett.*, vol. 6, no. 1, 2019, doi: 10.1186/s40562-019-0140-4.
19. S. Panchal and A. K. Shrivastava, “A comparative study of frequency ratio, shannon’s entropy and analytic hierarchy process (Ahp) models for landslide susceptibility assessment,” *ISPRS Int. J. Geo-Information*, vol. 10, no. 9, 2021, doi: 10.3390/ijgi10090603.
20. A. Jaafari, A. Najafi, H. R. Pourghasemi, J. Rezaeian, and A. Sattarian, “GIS-based frequency ratio and index of entropy models for landslide susceptibility assessment in the Caspian forest, northern Iran,” *Int. J. Environ. Sci. Technol.*, vol. 11, no. 4, pp. 909–926, 2014, doi: 10.1007/s13762-013-0464-0.
21. L. J. Wang, M. Guo, K. Sawada, J. Lin, and J. Zhang, “A comparative study of landslide susceptibility maps using logistic regression, frequency ratio, decision tree, weights of evidence and artificial neural network,” *Geosci. J.*, vol. 20, no. 1, pp. 117–136, 2016, doi: 10.1007/s12303-015-0026-1.
22. T. Melese, T. Belay, and A. Andemo, “Application of analytical hierarchal process, frequency ratio, and Shannon entropy approaches for landslide susceptibility mapping using geospatial technology: The case of Dejen district, Ethiopia,” *Arab. J. Geosci.*, vol. 15, no. 5, 2022, doi: 10.1007/s12517-022-09672-5.
23. A. Es-smairi, “Spatial prediction of landslide susceptibility using Frequency Ration (FR) and Shannon Entropy (SE) models : a case study from northern Rif , Morocco .,” 2022.
24. L. P. Sharma, N. Patel, M. K. Ghose, and P. Debnath, “Development and application of Shannon’s entropy integrated information value model for landslide susceptibility assessment and zonation in Sikkim Himalayas in India,” *Nat. Hazards*, vol. 75, no. 2, pp. 1555–1576, 2015, doi: 10.1007/s11069-014-1378-y.
25. N. Getachew and M. Meten, “Weights of evidence modeling for landslide susceptibility mapping of Kabi-Gebro locality, Gundomeskel area, Central Ethiopia,” *Geoenvironmental Disasters*, vol. 8, no. 1, p. 2022, 2021, doi: 10.1186/s40677-021-00177-z.
26. B. Pradhan, H. J. Oh, and M. Buchroithner, “Weights-of-evidence model applied to landslide susceptibility mapping in a tropical hilly area,” *Geomatics, Nat. Hazards Risk*, vol. 1, no. 3, pp. 199–223, 2010, doi: 10.1080/19475705.2010.498151.
27. M. H. Rezaei Moghaddam, M. Khayyam, M. Ahmadi, and M. Farajzadeh, “Mapping susceptibility landslide by using the weight-of-evidence model: A case study in Merek Valley, Iran,” *J. Appl. Sci.*, vol. 7, no. 22, pp. 3342–3355, 2007, doi: 10.3923/jas.2007.3342.3355.
28. Y. Cao, X. Wei, W. Fan, Y. Nan, W. Xiong, and S. Zhang, “Landslide susceptibility assessment using the Weight of Evidence method: A case study in Xunyang area, China,” *PLoS One*, vol. 16, no. 1 January, pp. 1–18, 2021, doi: 10.1371/journal.pone.0245668.

29. S. Lee and J. Choi, “Landslide susceptibility mapping using GIS and the weight-of-evidence model,” *Int. J. Geogr. Inf. Sci.*, vol. 18, no. 8, pp. 789–814, 2004, doi: 10.1080/13658810410001702003.
30. Q. Wang, W. Li, W. Chen, and H. Bai, “GIS-based assessment of landslide susceptibility using certainty factor and index of entropy models for the Qianyang county of Baoji city, China,” *J. Earth Syst. Sci.*, vol. 124, no. 7, pp. 1399–1415, 2015, doi: 10.1007/s12040-015-0624-3.
31. A. KEREKES, S. L. POSZET, and A. GÁL, “Landslide susceptibility assessment using the maximum entropy model in a sector of the Cluj–Napoca Municipality, Romania,” *Rev. Geomorfol.*, vol. 20, no. 1, pp. 130–146, 2018, doi: 10.21094/rg.2018.039.
32. M. S. Roodposhti, J. Aryal, H. Shahabi, and T. Safarrad, “Fuzzy Shannon entropy: A hybrid GIS-based landslide susceptibility mapping method,” *Entropy*, vol. 18, no. 10, 2016, doi: 10.3390/e18100343.
33. A. Kornejady, M. Ownegh, and A. Bahremand, “Landslide susceptibility assessment using maximum entropy model with two different data sampling methods,” *Catena*, vol. 152, pp. 144–162, 2017, doi: 10.1016/j.catena.2017.01.010.
34. T. Mersha and M. Meten, “GIS-based landslide susceptibility mapping and assessment using bivariate statistical methods in Simada area, northwestern Ethiopia,” *Geoenvironmental Disasters*, vol. 7, no. 1, 2020, doi: 10.1186/s40677-020-00155-x.
35. A. Genene, “Landslide Susceptibility Mapping Using GIS-based Information Value and Frequency Ratio Methods in Gindeberet area , West Shewa Zone , Oromia Region ,” 2021.
36. T. C. Korma, “GIS-based landslide susceptibility zonation mapping using frequency ratio and logistics regression models in the Dessie area , South Wello ,” pp. 1–25, 2022.
37. K. Solaimani, S. Z. Mousavi, and A. Kavian, “Landslide susceptibility mapping based on frequency ratio and logistic regression models,” *Arab. J. Geosci.*, vol. 6, no. 7, pp. 2557–2569, 2013, doi: 10.1007/s12517-012-0526-5.
38. S. Hidayat, H. Pachri, and I. Alimuddin, “Analysis of Landslide Susceptibility Zone using Frequency Ratio and Logistic Regression Method in Hambalang, Citeureup District, Bogor Regency, West Java Province,” *IOP Conf. Ser. Earth Environ. Sci.*, vol. 280, no. 1, 2019, doi: 10.1088/1755-1315/280/1/012005.
39. S. Lee and B. Pradhan, “Landslide hazard mapping at Selangor, Malaysia using frequency ratio and logistic regression models,” *Landslides*, vol. 4, no. 1, pp. 33–41, 2007, doi: 10.1007/s10346-006-0047-y.
40. G. Das and K. Lepcha, “Application of logistic regression (LR) and frequency ratio (FR) models for landslide susceptibility mapping in Relli Khola river basin of Darjeeling Himalaya, India,” *SN Appl. Sci.*, vol. 1, no. 11, pp. 1–22, 2019, doi: 10.1007/s42452-019-1499-8.
41. C. Sivakami and Dr. R. Rajkumar, “Landslide Vulnerability Zone by Weights of Evidence Model using Remote Sensing and GIS, in Kodaikanal Taluk (Tamil nadu, India),” *Int. J. Eng. Res.*, vol. V9, no. 02, pp. 788–793, 2020, doi: 10.17577/ijertv9is020201.
42. A. Wubalem, “Modeling of Landslide susceptibility in a part of Abay Basin, northwestern Ethiopia,” *Open Geosci.*, vol. 12, no. 1, pp. 1440–1467, 2020, doi: 10.1515/geo-2020-0206.
43. B. Pradhan, S. Lee, and M. F. Buchroithner, “Remote sensing and GIS-based landslide susceptibility analysis and its cross-validation in three test areas using a frequency ratio model,” *Photogramm. Fernerkundung, Geoinf.*, vol. 2010, no. 1, pp. 17–32, 2010, doi: 10.1127/1432-8364/2010/0037.
44. A. Wubalem, “Landslide susceptibility mapping using statistical methods in Uatzau catchment area, northwestern Ethiopia,” *Geoenvironmental Disasters*, vol. 8, no. 1, pp. 1–21, 2021, doi: 10.1186/s40677-020-

00170-y.

45. L. Ayalew and H. Yamagishi, “The application of GIS-based logistic regression for landslide susceptibility mapping in the Kakuda-Yahiko Mountains, Central Japan,” *Geomorphology*, vol. 65, no. 1–2, pp. 15–31, 2005, doi: 10.1016/j.geomorph.2004.06.010.
46. G. liang Du, Y. shuang Zhang, J. Iqbal, Z. hua Yang, and X. Yao, “Landslide susceptibility mapping using an integrated model of information value method and logistic regression in the Bailongjiang watershed, Gansu Province, China,” *J. Mt. Sci.*, vol. 14, no. 2, pp. 249–268, 2017, doi: 10.1007/s11629-016-4126-9.
47. B. T. Pham *et al.*, “A novel ensemble classifier of rotation forest and Naïve Bayer for landslide susceptibility assessment at the Luc Yen district, Yen Bai Province (Viet Nam) using GIS,” *Geomatics, Nat. Hazards Risk*, vol. 8, no. 2, pp. 649–671, 2017, doi: 10.1080/19475705.2016.1255667.
48. C. Xu, F. Dai, X. Xu, and Y. H. Lee, “GIS-based support vector machine modeling of earthquake-triggered landslide susceptibility in the Jianjiang River watershed, China,” *Geomorphology*, vol. 145–146, pp. 70–80, 2012, doi: 10.1016/j.geomorph.2011.12.040.
49. H. Shu, Z. Guo, S. Qi, D. Song, H. R. Pourghasemi, and J. Ma, *Integrating landslide typology with weighted frequency ratio model for landslide susceptibility mapping: A case study from lanzhou city of northwestern china*, vol. 13, no. 18. 2021. doi: 10.3390/rs13183623.
50. S. He, P. Pan, L. Dai, H. Wang, and J. Liu, “Application of kernel-based Fisher discriminant analysis to map landslide susceptibility in the Qinggan River delta, Three Gorges, China,” *Geomorphology*, vol. 171–172, pp. 30–41, 2012, doi: 10.1016/j.geomorph.2012.04.024.
51. H. Khan, M. Shafique, M. A. Khan, M. A. Bacha, S. U. Shah, and C. Calligaris, “Landslide susceptibility assessment using Frequency Ratio, a case study of northern Pakistan,” *Egypt. J. Remote Sens. Sp. Sci.*, vol. 22, no. 1, pp. 11–24, 2019, doi: 10.1016/j.ejrs.2018.03.004.
52. N. R. Regmi, J. R. Giardino, and J. D. Vitek, “Modeling susceptibility to landslides using the weight of evidence approach: Western Colorado, USA,” *Geomorphology*, vol. 115, no. 1–2, pp. 172–187, 2010, doi: 10.1016/j.geomorph.2009.10.002.
53. C. Y. Chen and F. C. Yu, “Morphometric analysis of debris flows and their source areas using GIS,” *Geomorphology*, vol. 129, no. 3–4, pp. 387–397, 2011, doi: 10.1016/j.geomorph.2011.03.002.
54. S. Karim, S. Jalileddin, and M. T. Ali, “Zoning Landslide by Use of Frequency Ratio Method (Case Study: Deylaman Region),” vol. 9, no. 5, pp. 578–583, 2011.
55. S. Mohsen Mousavi, A. Golkarian, S. Amir Naghibi, B. Kalantar, and B. Pradhan, “GIS-based Groundwater Spring Potential Mapping Using Data Mining Boosted Regression Tree and Probabilistic Frequency Ratio Models in Iran,” *AIMS Geosci.*, vol. 3, no. 1, pp. 91–115, 2017, doi: 10.3934/geosci.2017.1.91.
56. D. Sarkar, S. Saha, and P. Mondal, “GIS-based frequency ratio and Shannon’s entropy techniques for flood vulnerability assessment in Patna district, Central Bihar, India,” *Int. J. Environ. Sci. Technol.*, no. 3000609305, p. 2022, 2021, doi: 10.1007/s13762-021-03627-1.
57. S. Lee and J. A. Talib, “Probabilistic landslide susceptibility and factor effect analysis,” *Environ. Geol.*, vol. 47, no. 7, pp. 982–990, 2005, doi: 10.1007/s00254-005-1228-z.
58. A. D. Regmi, K. Yoshida, H. R. Pourghasemi, M. R. DhitaL, and B. Pradhan, “Landslide susceptibility mapping along Bhalubang — Shiwapur area of mid-Western Nepal using frequency ratio and conditional probability models,” *J. Mt. Sci.*, vol. 11, no. 5, pp. 1266–1285, 2014, doi: 10.1007/s11629-013-2847-6.

59. A. Haghizadeh, S. Siahkamari, A. H. Haghiabi, and O. Rahmati, “Forecasting flood-prone areas using Shannon’s entropy model,” *J. Earth Syst. Sci.*, vol. 126, no. 3, 2017, doi: 10.1007/s12040-017-0819-x.
60. F. Guzzetti, “Landslide hazard assessment and risk evaluation: limits and prospectives,” *Proc. 4th EGS Plinius Conf.*, no. October 2002, pp. 1–4, 2003.
61. E. Yesilnacar and T. Topal, “Landslide susceptibility mapping: A comparison of logistic regression and neural networks methods in a medium scale study, Hendek region (Turkey),” *Eng. Geol.*, vol. 79, no. 3–4, pp. 251–266, 2005, doi: 10.1016/j.enggeo.2005.02.002.
62. T. Fawcett, “An introduction to ROC analysis,” *Pattern Recognit. Lett.*, vol. 27, no. 8, pp. 861–874, 2006, doi: 10.1016/j.patrec.2005.10.010.

Figures

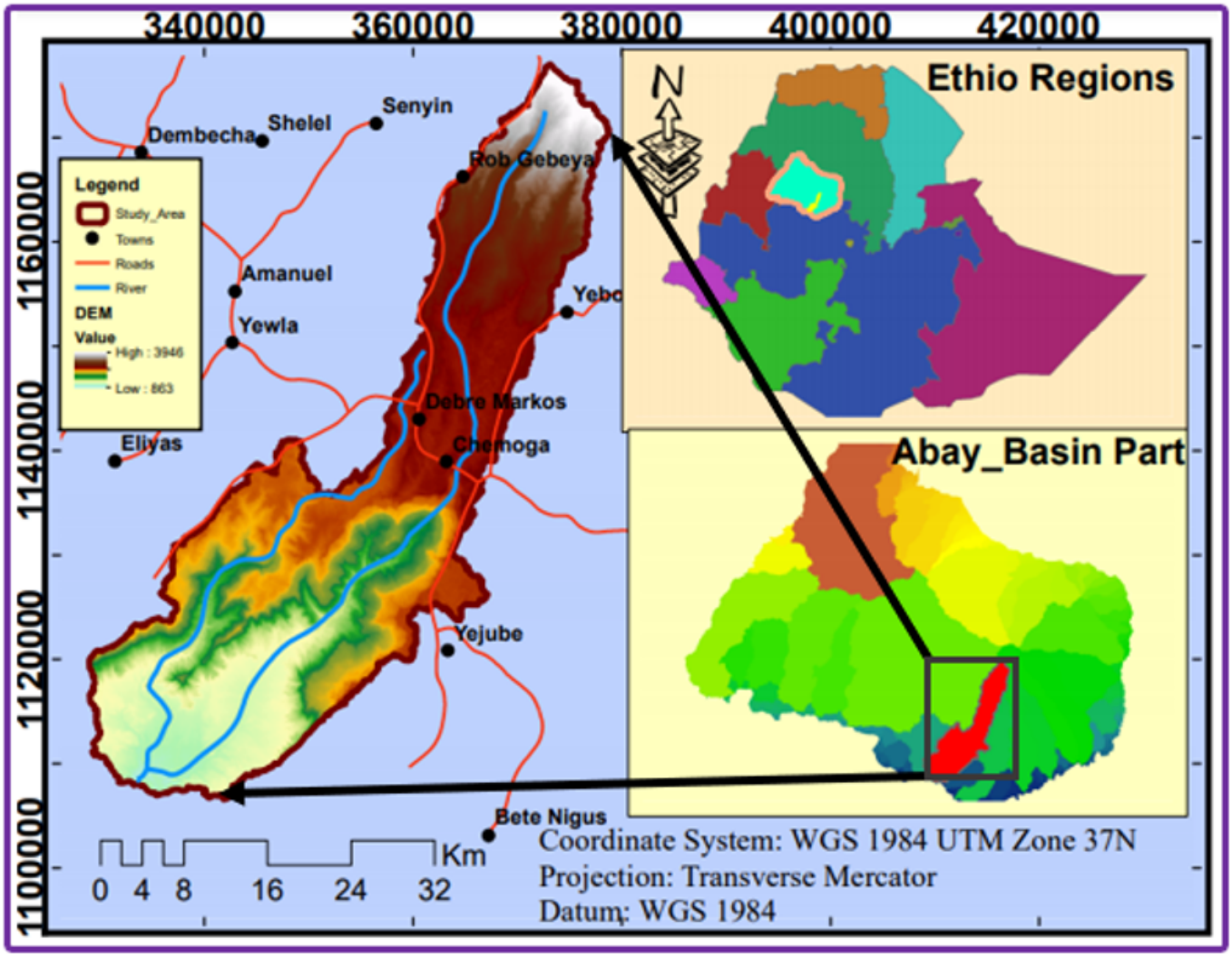

Figure 1

Location map of study area

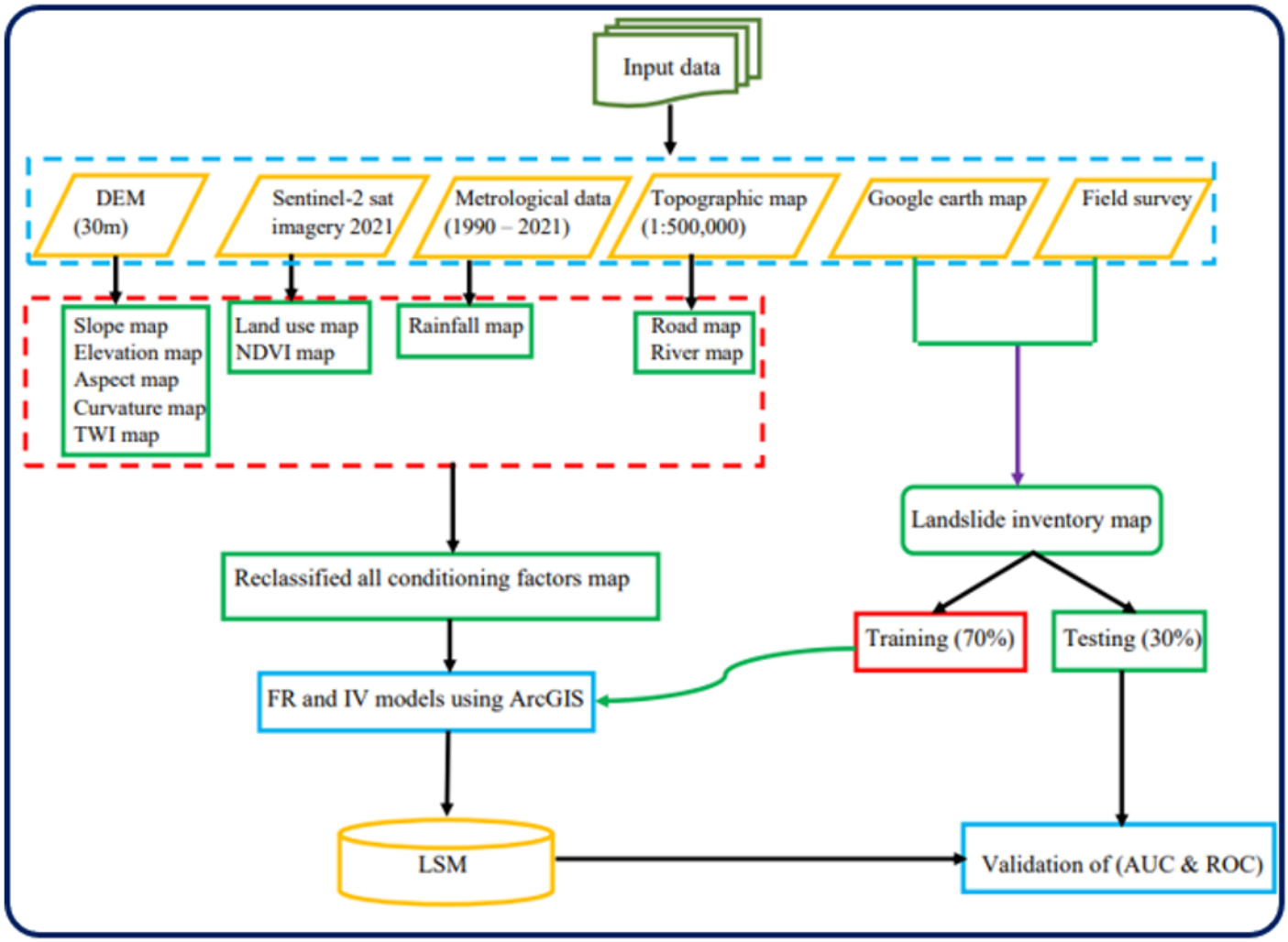

Figure 2

Workflow of the methodology

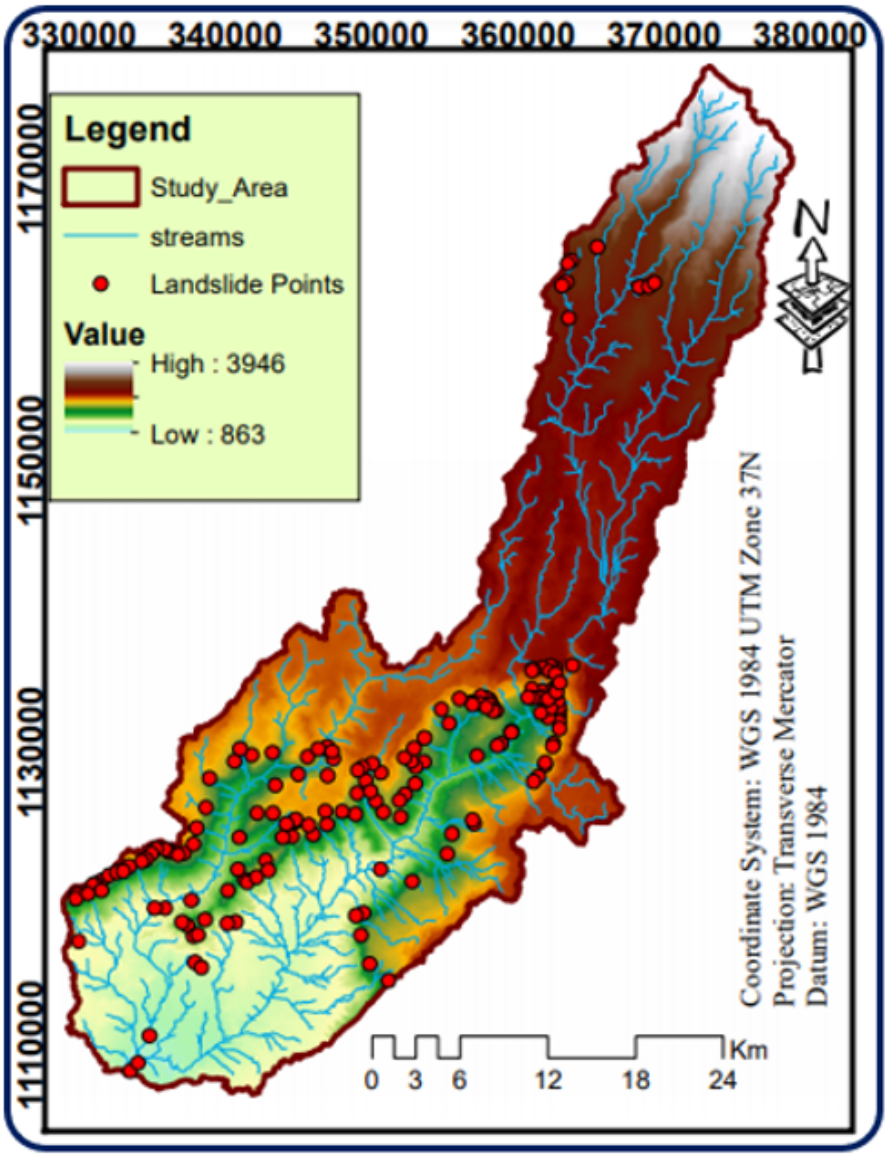

Figure 3

Landslide inventory map

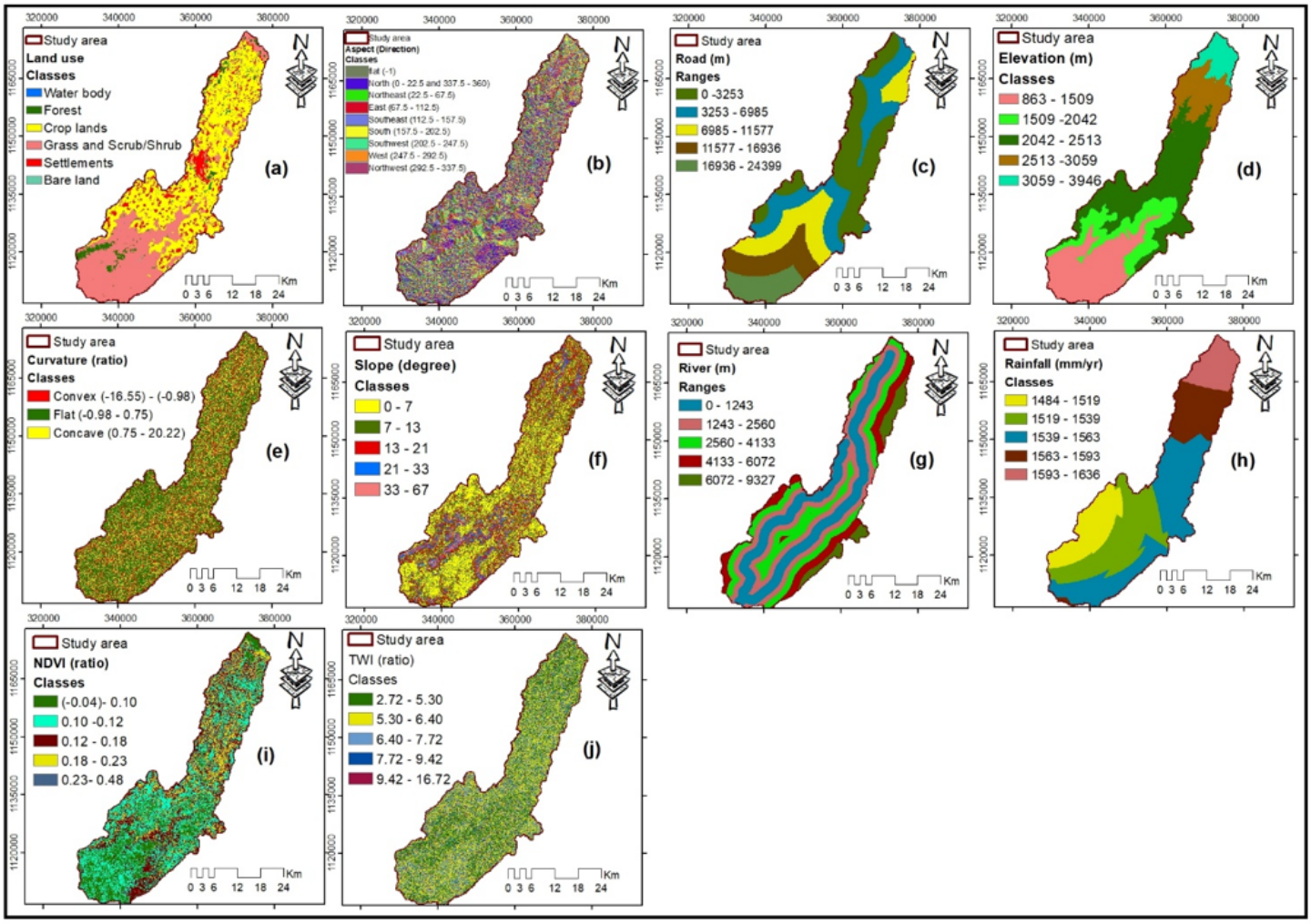

Figure 4

Landslide conditioning factors; (**a**) Land use (**b**) Aspect (**c**) Road (**d**) Elevation (**e**) Curvature (**f**) Slope (**g**) River (**h**) Rainfall (**i**) NDVI and (**j**) TWI

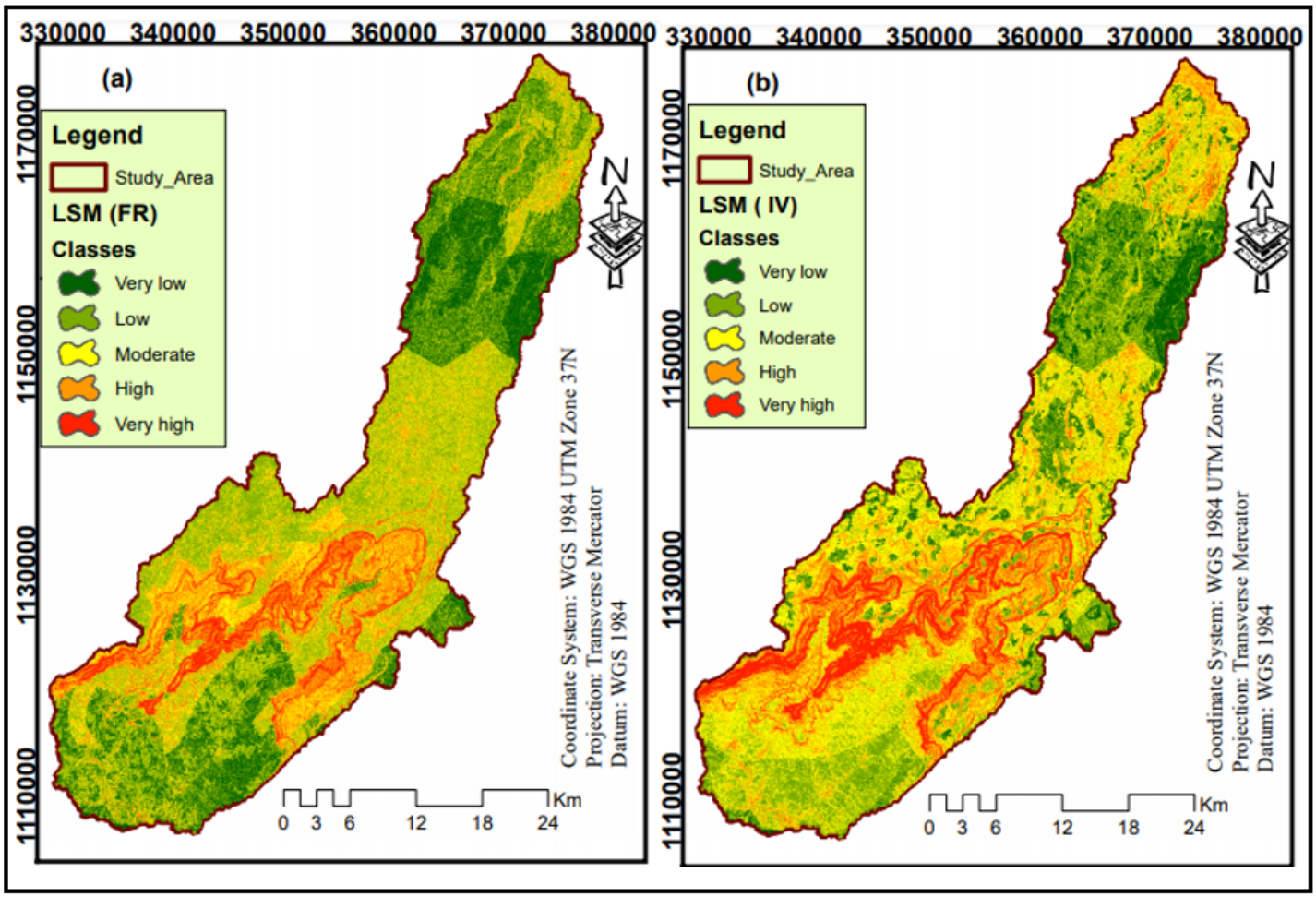

Figure 5

Landslide susceptibility map using (**a**) Frequency Ratio (FR) and (**b**) Information Values (IV) models

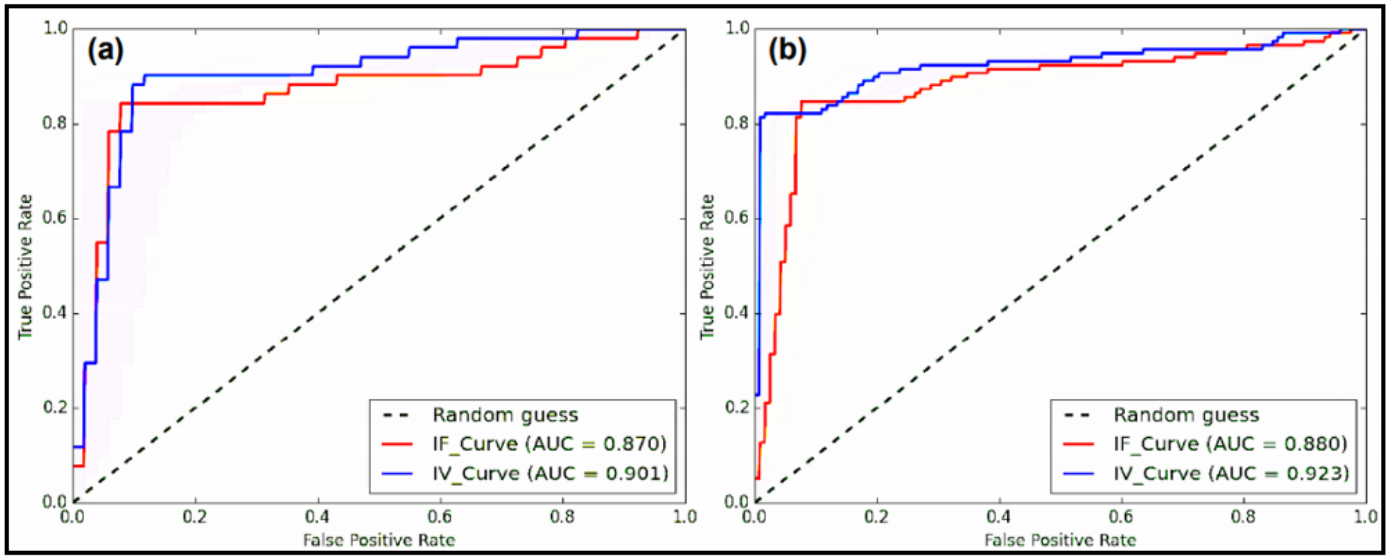

Figure 6

The AUC of success rate curve (a) and predication rate curve (b) both FR and IV models